J Physiol 589.23 (2011) pp 5801–5818

The Journal of Physiology

Processing of central and reflex vagal drives by rat cardiac ganglion neurones: an intracellular analysis

Robin M. McAllen[1], Lauren M. Salo[2], Julian F. R. Paton[2] and Anthony E. Pickering[2]

[1] *Florey Neuroscience Institutes and Department of Anatomy & Cell Biology, University of Melbourne, Melbourne, Victoria 3010, Australia*
[2] *School of Physiology and Pharmacology, Bristol Heart Institute, Medical Sciences Building, University Walk, University of Bristol, Bristol BS8 1TD, UK*

Non-technical summary The brain controls the heart through parasympathetic (vagal) and sympathetic nerves. Vagal control is integral to cardiac health and a loss of vagal tone is a poor prognostic sign in cardiovascular diseases such as heart failure and hypertension. The vagal drive to the heart is transmitted across synapses located in the cardiac ganglia on the heart. We have developed a novel methodology to make intracellular recordings from cardiac ganglion neurones on the surface of the beating heart in a preparation with intact functional drive from the brainstem. We show how these neurones process their synaptic inputs and demonstrate that the ganglion plays a key role in regulating the level of vagal tone reaching the heart. This identifies the cardiac ganglion as a viable target for interventions to restore the transmission of vagal tone in cardiovascular diseases.

Abstract Cardiac vagal tone is an important indicator of cardiovascular health, and its loss is an independent risk factor for arrhythmias and mortality. Several studies suggest that this loss of vagal tone can occur at the cardiac ganglion but the factors affecting ganglionic transmission *in vivo* are poorly understood. We have employed a novel approach allowing intracellular recordings from functionally connected cardiac vagal ganglion cells in the working heart–brainstem preparation. The atria were stabilised *in situ* preserving their central neural connections, and ganglion cells ($n = 32$) were impaled with sharp microelectrodes. Cardiac ganglion cells with vagal synaptic inputs (spontaneous, $n = 10$; or electrically evoked from the vagus, $n = 3$) were identified as principal neurones and showed tonic firing responses to current injected to their somata. Cells lacking vagal inputs ($n = 19$, presumed interneurones) were quiescent but showed phasic firing responses to depolarising current. In principal cells the ongoing action potentials and EPSPs exhibited respiratory modulation, with peak frequency in post-inspiration. Action potentials arose from unitary EPSPs and autocorrelation of those events showed that each ganglion cell received inputs from a single active preganglionic source. Peripheral chemoreceptor, arterial baroreceptor and diving response activation all evoked high frequency synaptic barrages in these cells, always from the same single preganglionic source. EPSP amplitudes showed frequency dependent depression, leading to more spike failures at shorter inter-event intervals. These findings indicate that rather than integrating convergent inputs, cardiac vagal postganglionic neurones gate preganglionic inputs, so regulating the proportion of central parasympathetic tone that is transmitted on to the heart.

(Received 20 June 2011; accepted after revision 10 October 2011; first published online 17 October 2011)
Corresponding author A. E. Pickering: School of Physiology and Pharmacology, Bristol Heart Institute, Medical Sciences Building, University Walk, University of Bristol, Bristol BS8 1TD, UK. Email: tony.pickering@bristol.ac.uk

Abbreviations: AHP, after-hyperpolarisation; HR, heart rate; PNA, phrenic nerve activity; PP, perfusion pressure; SAH, slow after-hyperpolarisation; V_m, membrane potential; WHBP, working heart–brainstem preparation.

J. F. R. Paton and A. E. Pickering are joint last authors.

DOI: 10.1113/jphysiol.2011.214320

Introduction

The ganglionic synapse represents the final neural processing stage in the cardiac vagal pathway before the neuroeffector junction at the heart. As such, it provides an important site where neural activity may be modulated or controlled. One view of synaptic function at this site, based in part on *in vitro* recordings (Selyanko & Skok, 1992; Rimmer & Harper, 2006) and on comparisons with other parasympathetic ganglia (Melnitchenko & Skok, 1970; Lichtman, 1977), proposes that ganglionic transmission of vagal impulses is predominantly secure with a large safety margin, and that this site is therefore largely a relay for centrally generated tone. A second perspective of the ganglion posits that it forms a 'cardiac brain' with different classes of local integrative circuit neurones (Steele *et al.* 1994; Edwards *et al.* 1995; Richardson *et al.* 2003; and see review Armour, 2008) much like the organisation of the enteric nervous system. The implication of this viewpoint is that the synaptic transmission of vagal impulses may be modulated or supplemented by the local ganglionic circuits and also by circulating/paracrine factors. In considering these models it is important to note that there is evidence for severe impairment of vagal ganglionic transmission in rats with hypertension (Heaton *et al.* 2007) and in dogs with experimentally induced heart failure (Bibevski & Dunlap, 1999) accompanied by changes in ganglion cell excitability (Arora *et al.* 2003), which are proposed to account for the loss of vagal tone seen in these conditions. This raises the question of how vagal transmission works *in vivo* both in health and in disease states.

The cardiac vagal postganglionic neurones are located in ganglionic plexi on the heart and there is evidence indicating that each plexus may exert differential (but overlapping) influences on aspects of cardiac function (i.e. chronotropism and dromotropism; see Sampaio *et al.* 2003). Valuable functional insights have been obtained from extracellular recordings made *in vivo* (Armour *et al.* 1998) and intracellular recordings from *in vitro* preparations (e.g. Selyanko & Skok, 1992; Edwards *et al.* 1995; Rimmer & Harper, 2006). However, no intracellular study has yet been able to show how cardiac ganglion cells integrate their physiological inputs and generate the postganglionic motor activity destined for the heart, at least in part because cardiac motion has made microelectrode recordings challenging. Using the working heart–brainstem preparation (Paton, 1996), we have been able to make intracellular recordings from functionally connected cardiac vagal ganglion cells *in situ* (some of these data have previously been communicated to the Physiological Society; Pickering *et al.* 2009). We now report the first study of how cardiac ganglion cells process and transmit physiologically generated synaptic inputs.

Methods

Ethical approvals

All experiments conformed strictly to the UK Home Office guidelines regarding the ethical use of animals and were approved by the Home Office and the University of Bristol's ethical review committee.

Working heart–brainstem preparation. The working heart–brainstem preparation (WHBP) was established using previously described methods (see Fig. 1; Paton, 1996). In brief, male Wistar rats ($n = 6$, 24–36 days postnatal) were deeply anaesthetised with halothane, until loss of paw withdrawal to pinch. The rat was then bisected subdiaphragmatically, exsanguinated, cooled in carbogenated Ringer solution at 5–10°C, and suction-decerebrated pre-collicularly, after which the halothane anaesthesia was discontinued. The preparation was kept cold while the phrenic nerve and descending aorta were dissected free, and a bilateral pneumonectomy was performed. The ventricles were removed taking care to leave the aortic valve intact. The rib cage and spinal column were transected at T5 to facilitate access to the atria.

A bipolar stimulating electrode was placed on the intact right cervical vagus nerve ($n = 4$ preparations). This consisted of two fine, Teflon-insulated silver wires that were bared at their point of contact with the nerve. These were threaded on a loom 1 mm apart (silicone tubing longitudinally bisected) that was placed in contact with the vagus nerve, insulated with paraffin oil and polythene film, then stabilised in place with low melting point wax. Stimuli were applied to the vagus nerve from an isolated voltage stimulator (5–20 V, 1 ms, 0.5–2 Hz).

After transfer to the recording chamber, a double lumen cannula was inserted into the descending aorta for retrograde perfusion with carbogen-gassed modified Ringer solution (see below for composition) containing Ficoll-70 (1.25%; Sigma) at 32°C. The perfusate was pumped from a reservoir flask, via a heat exchanger, through two bubble traps and a particle filter (25 μm screen, Millipore) before passing via the cannula to the preparation. It was then recycled from the preparation chamber back to the reservoir for carbogenation and re-warming. Flow was generated with a peristaltic pump (Watson-Marlow 505D, Falmouth, Cornwall, UK) with a maintained volume in the circuit of ~200 ml. The perfusion pressure was monitored via the second lumen of the cannula.

The heart resumed beating almost immediately as the perfusate flow was gradually increased to a typical basal flow of 25 ml min^{-1}. As the preparation warmed up, rhythmic respiratory muscle contractions were seen after 1–3 min, signalling the return of brainstem function. At this point muscle relaxant was added to

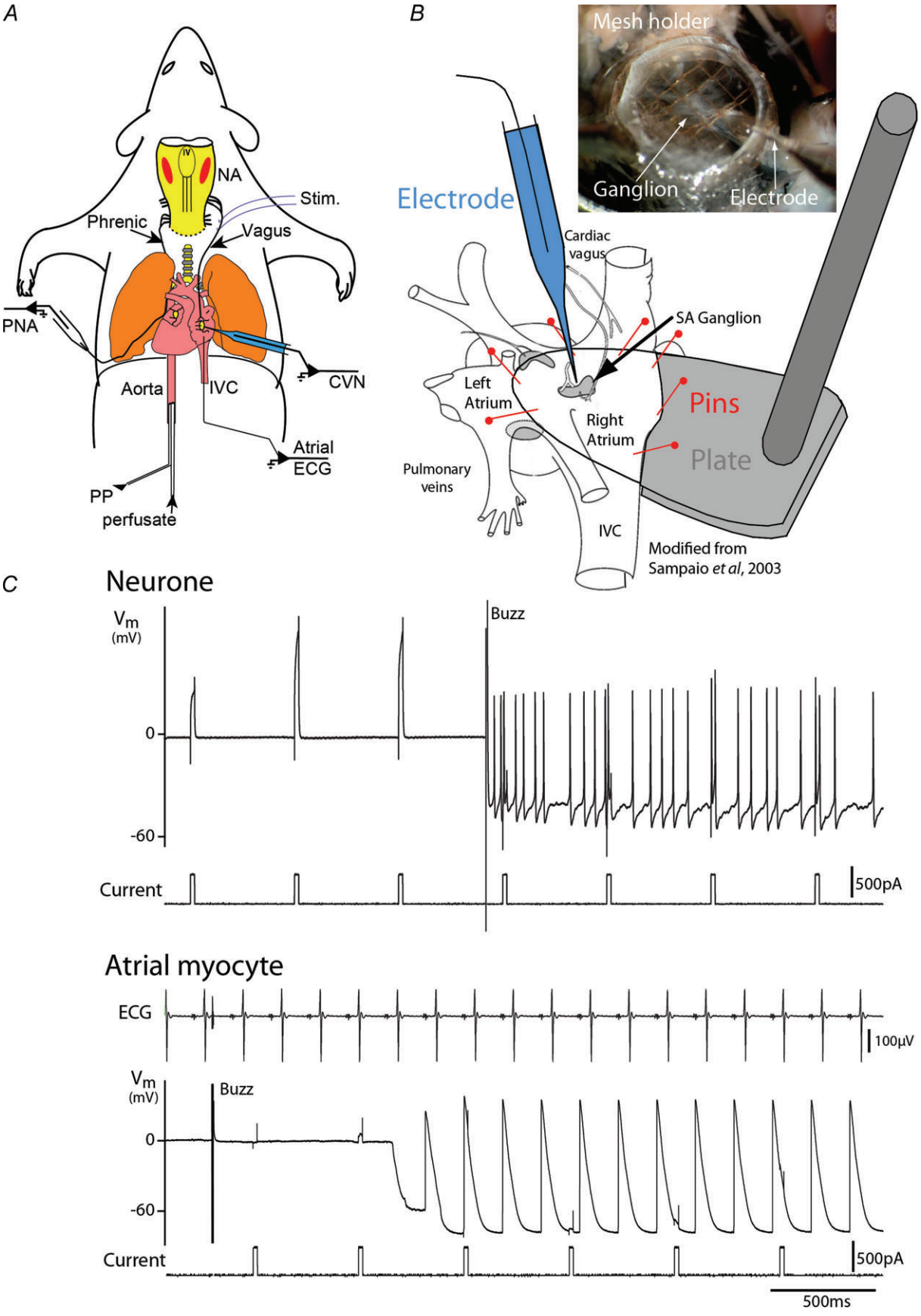

the perfusion solution (Vecuronium 200 μg; Norcuron, Organon, Cambridge, UK). The preparation was held in ear bars and positioned prone to allow access to the dorsal aspect of the atria. The inferior vena cava was identified and traced up to the right atrium. An incision was then made in the lateral aspect of the inferior vena cava and extended into the right atrium to admit a Sylgard-covered footplate. The dorsal surface of the atrium was pinned over the plate using insect pins. The central portion of the pinned atrium was further stabilised with a nylon mesh glued to a section of hypodermic needle attached to a 3-D micro-manipulator. Beneath the mesh the ganglia and associated nerves were visible under a dissecting microscope (see Fig. 1) and atrial contractions were visible.

Phrenic nerve recordings. The phrenic nerve was recorded using a monopolar suction electrode allowing both phrenic activity and ECG to be recorded simultaneously. An additional silver wire electrode was inserted to the inferior vena cava to record atrial ECG in some experiments. The signals were AC amplified (10–20 k) and bandpass filtered (80 Hz to 3 kHz). A window discriminator was used to trigger from the ECG to derive instantaneous heart rate. Rhythmic, ramping phrenic nerve activity (PNA) gave a continuous physiological index of preparation viability. During the initial phase of each experiment the preparation was tuned to obtain a robust eupnoeic pattern of PNA by fine adjustment of perfusate flow rate and/or the addition of arginine-vasopressin to the reservoir (200–400 pM). Once established with a ramping eupnoeic pattern, with the consequent engagement of respiratory–sympathetic coupling, which acted to increase the vascular tone, the preparation usually required little further adjustment during the remainder of the experiment (typically 2–4 h).

Cardiac ganglion cell intracellular recordings. The sinoatrial node ganglion was identified on the epicardial surface of the right atrium by reference to the convergence of nerve fibres coursing over its surface, lateral to the pulmonary veins entering the left atrium (Fig. 1*B*). Sharp microelectrodes were pulled from borosilicate capillary glass (Harvard Clark GC150-F10) and had resistances of 60–100 MΩ when filled with 0.5 M KCl. The electrodes were advanced using a water hydraulic manipulator (Narishige) at an oblique angle into the ganglion and neurones were impaled using the buzz function on the amplifier (Axoclamp 2B, Axon Instruments). Successful penetration was indicated by the presence of a resting potential more negative than –30 mV and by the presence of overshooting action potentials with durations of less than 10 ms (which distinguished the neurones from atrial myocytes, see Fig. 1*C*). Stable recordings were obtained for periods of up to 40 min and were reliably maintained during robust cardio-respiratory reflex activations that caused substantial bradycardias. Following a successful recording it was sometimes possible to advance a short distance (20–30 μm) and obtain a further neuronal recording; however, further advancement often resulted in the impalement of an atrial myocyte (easily recognised by their distinctive action potential morphology; Fig. 1*C*) consistent with the epithelial arrangement of the cardiac ganglia (see Rimmer & Harper, 2006). Thus, the impalement of atrial myocytes provided a useful indication of the electrode position relative to the neuro-epithelium.

Cardio-respiratory reflex activation. Peripheral chemoreceptors were stimulated using intra-arterial injection of sodium cyanide (50–100 μl of 0·03%) as a bolus into the perfusion line. The chemoreflex responses were dose dependent and the doses used produced submaximal bradycardia (1–2 Hz decrease in frequency) and increased phrenic burst rate.

The diving response was evoked by application of cold Ringer solution (~10°C, 50–200 μl) to the snout, which triggered a characteristic apnoea and bradycardia.

Figure 1. Approach to the sinoatrial cardiac ganglion in the working heart–brainstem preparation
A, Wistar rats (aged 24–36 days) were anaesthetised with halothane, decerebrated pre-collicularly and perfused through the ascending aorta with carbogenated Ringer solution (32°C) containing Ficoll. Phrenic nerve activity (PNA) and atrial electrocardiogram (ECG) were recorded. Cardiac vagal ganglion neurones (CVN) were functionally characterised by their response to activation of peripheral chemoreceptors (NaCN, 0.03% I.A.), arterial baroreceptors (increased perfusion pressure) and diving response (cold saline to snout). A bipolar stimulating electrode (stim) was placed in contact with the right cervical vagus. PP – perfusion pressure, NA – nucleus ambiguus, IVC – inferior vena cava. *B*, to allow stable intracellular recordings, the ventricles were removed, the right atrium was opened along its lateral aspect and the inter-atrial septum cut open. A stabilising, Sylgard-coated footplate was inserted into the open atria and the muscle was pinned to its surface (figure adapted from Sampaio *et al.* 2003). A mesh grid was lowered onto the atrial tissue for further stabilisation while permitting visualisation of the cardiac ganglia (shown schematically in grey, SA – sinoatrial) located on the epicardial surface (inset photograph). *C*, sharp microelectrode recordings were obtained from 32 cardiac ganglion neurones (V_m – membrane potential). These recordings proved remarkably stable, lasting for up to 40 min often allowing multiple cardio-respiratory reflex activations. They were easily distinguished from the underlying atrial myocytes (lower trace) on the basis of action potential shape and entrainment with ECG.

The arterial baroreflex was activated by increasing transiently the flow from the pump (2–5 s) to generate a perfusion pressure ramp of 20–50 mmHg, which evoked a characteristic bradycardia.

Data recording and analysis. Perfusion pressure, ECG and PNA were recorded using custom built AC amplifiers and transducers (Physiology and Pharmacology Electronic workshop, University of Bristol) and collected via an A-D interface (micro1401, CED, Cambridge, UK) to a computer running Spike2 software (CED). Custom scripts were used for data acquisition and analysis in Spike2.

Autocorrelation of synaptic events. Neurones showing ongoing action potentials were hyperpolarised to prevent action potential discharge. Using the 'slope' function in Spike2, the membrane potential recording of ongoing synaptic activity was differentiated. From this differentiated signal the individual EPSPs were discriminated. This method distinguishes individual synaptic events even when EPSPs summate (Bratton *et al.* 2010). The minimum detectable separation was set at 1 ms. Autocorrelation histograms (autocorrelograms) were then generated from these data, using Spike2. This process iteratively takes each event in a time series as the reference (trigger) time, and sets a time window either side that reference time. All other events within that time window are counted and plotted on a histogram whose x-axis represents time relative to the trigger event. Then the next event is set as the trigger and the process is repeated, accumulating counts on the histogram. (N.B. the same event may be counted more than once.) The logic of using the autocorrelogram to detect single unit inputs has been discussed elsewhere (Bratton *et al.* 2010). Briefly, it relies on the fact that subsynaptic events such as EPSPs have no refractory period, but the action potentials in presynaptic neurons are all-or-nothing events with absolute refractory periods. When a single presynaptic neuron is driving all EPSPs, its refractory period will set a minimum time between successive EPSPs, which is manifest as a central gap in the autocorrelogram. When two or more presynaptic neurons are driving the EPSPs, the random coincidences between their arrival times will show no minimum interval, giving no central gap in the autocorrelogram. To demonstrate this principle, a double input was simulated from real data by the following method. Events from the second minute of a 2 min record were superimposed on those from the first minute, and the timescale stretched twofold to restore the original mean event rate. The autocorrelation from this simulated double input could then be compared with the original recorded autocorrelogram.

Statistical analysis. Unless otherwise stated data were expressed as means ± standard error of the mean. n refers to the number of cells. Student's two-tailed t test was used to establish statistical significance of differences between sampled populations (Prism 5, Graphpad Software, San Diego, CA, USA). Least squares linear regression was used to determine the influence of the preceding

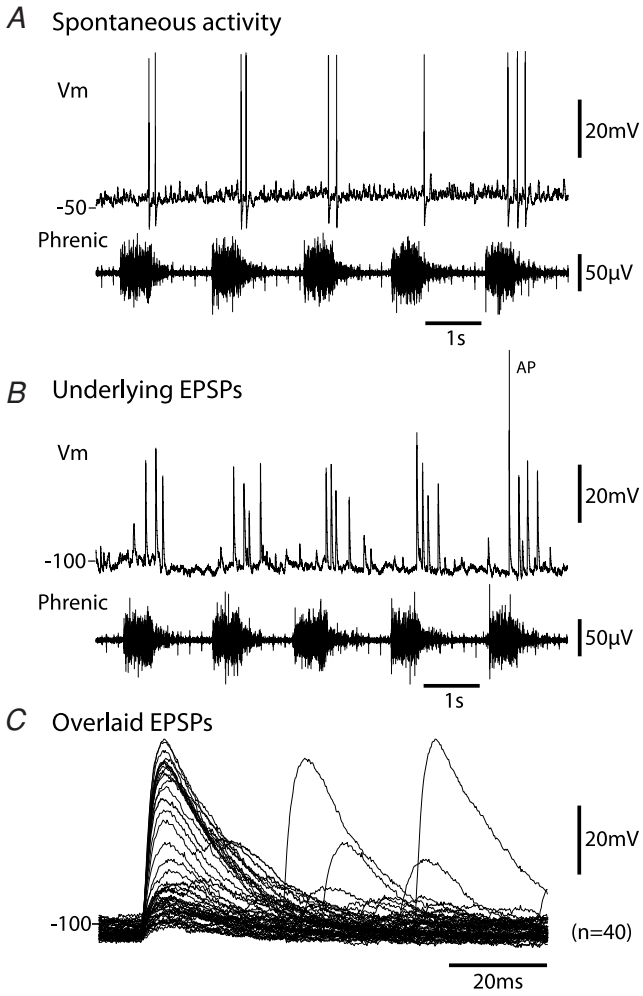

Figure 2. Spontaneous activity of cardiac ganglion neurones
A, characteristic recording from a cardiac ganglion neurone showing the spontaneous discharge of action potentials. Note these were entrained to the postinspiratory phase of the respiratory cycle (see alignment with phrenic nerve activity below) as would be expected for cardiac 'vagal tone'. *B*, injection of hyperpolarising current demonstrated these action potentials were driven by large EPSPs that were suprathreshold (unless the membrane was driven to hyperpolarised potentials) and occurred in the postinspiratory phase. *C*, these spontaneous EPSPs had a fast time to peak of 5 ms and a decay time constant of 18 ms. The smaller subthreshold events followed a similar time course as shown in the overlaid trace showing 40 consecutive events. Although some temporal summation of EPSPs was seen, it was relatively uncommon and did not appear to contribute to action potential discharge under basal conditions. (Note the monopolar phrenic nerve recording also includes the ECG signal.)

interval on EPSP amplitude, and whether the slope of the relation differed significantly from zero (Microsoft Excel). Statistical significance was defined as $P < 0.05$.

Drugs and solutions. The composition of the modified Ringer solution was (mM): NaCl (125); $NaHCO_3$ (24); KCl (3); $CaCl_2$ (2.5); $MgSO_4$ (1.25); KH_2PO_4 (1.25); dextrose (10); pH 7.35–7.4 after carbogenation. All chemicals were from Sigma (UK).

Results

Stable intracellular recordings were obtained from 32 cardiac ganglion neurones with a resting membrane potential of -44.5 ± 1.8 mV. The cells fell into two categories: those with vagally evoked or spontaneous postsynaptic activity that could produce action potential discharge ($n = 13$, Fig. 2*A*) and quiescent neurones with no spontaneous action potential discharge and either no synaptic activity or very sporadic, small subthreshold synaptic events ($n = 19$).

Spontaneous activity in cardiac ganglion cells

Ten neurones showed ongoing synaptic activity and six of these showed spontaneous action potentials (0.2–4.3 Hz, $n = 6$, Fig. 2*A*) which were driven by single suprathreshold EPSPs (Fig. 2*B* and *C*, revealed by the injection of hyperpolarising current to prevent spiking). In these neurones the spontaneous EPSPs had a mean frequency of 4.1 ± 0.7 Hz with amplitude of 10.1 ± 3.3 mV ($n = 6$ cells, over 30 s of spontaneous activity). This activity showed a clear pattern of respiratory modulation (see Fig. 2*A* and *B*). When the ongoing synaptic events were plotted as phrenic cycle-triggered event histograms the peak activity occurred in post-inspiration in all cases (see Fig. 3, in agreement with the timing of cardiac vagal bursts that are seen in the rat WHBP; Simms *et al.* 2007). The postinspiratory peak sometimes began in late inspiration (cf. Rentero *et al.* 2002), but activity was always minimal in early inspiration (Fig. 3). No IPSPs were observed in these cells under either resting or hyperpolarised conditions.

Injection of depolarising current pulses sufficient to reach threshold showed these active cells ($n = 3/3$ tested) to have a tonic pattern of spike discharge (see Fig. 4*A*), analogous to the slow after-hyperpolarisation (SAH) cells that were reported, on the basis of *in vitro* studies, to be the principal neurones of the cardiac ganglion (Edwards *et al.* 1995). On the basis that these neurones had a pattern of respiratory modulated spontaneous activity that would be anticipated for cardiac vagal tone generating

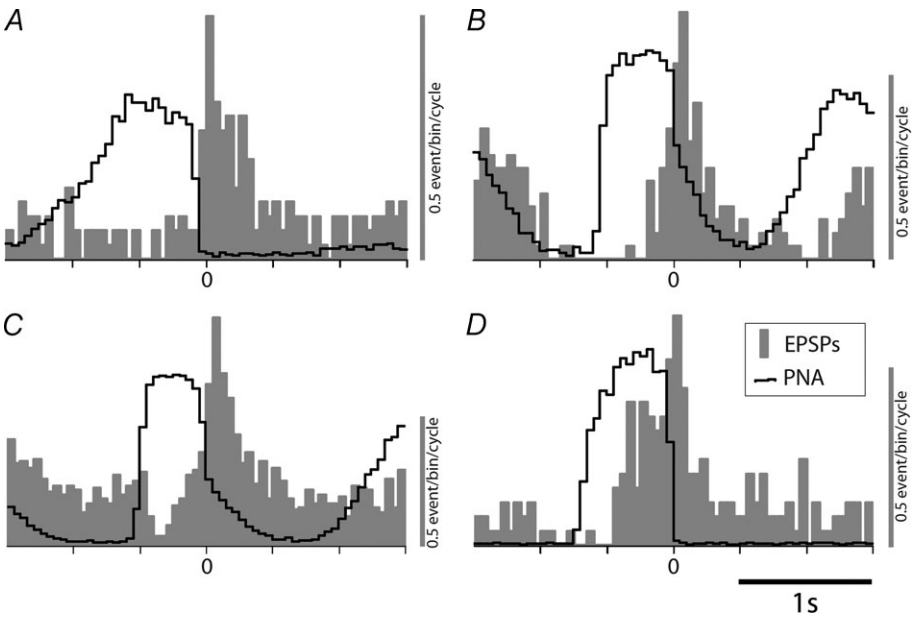

Figure 3. Respiratory modulation of spontaneous synaptic event frequency in the cardiac ganglion principal cells
The frequency of occurrence of the EPSPs was seen to be strongly respiratory modulated in all cases tested (9/9). The figure shows 4 representative respiratory cycle-triggered event histograms (aligned at start of postinspiratory phase) from neurones recorded in four different preparations. All show a peak of synaptic activity during the early postinspiratory phase of the respiratory cycle. The respiratory-related synaptic barrage often started during the late phase of inspiration but the trough of EPSP occurrence was always at the start of inspiration (*A–D*). Grey bars represent synaptic event frequency in 50 ms bins vertical grey scale – 0.5 event/bin. The black trace shows integrated phrenic nerve activity (in arbitrary units).

respiratory sinus arrhythmia they are henceforth referred to as principal cells.

Quiescent cells

These neurones ($n = 19$) had stable resting membrane potentials of -45.8 ± 2.8 mV, with either no synaptic activity or very sporadic, small (<5 mV) subthreshold synaptic events (Fig. 4*B*). Action potential discharge could be evoked by the injection of depolarising current. However, these cells showed a strongly accommodating pattern of discharge ($n = 13/13$ tested) and often only fired a single spike (or occasionally a doublet). These cells correspond to the phasic cells reported in guinea pig cardiac ganglion *in vitro* (Edwards *et al.* 1995), which have been presumed to be interneurones of the cardiac ganglion.

Principal cell excitatory responses to cardio-respiratory reflex activation

Ganglion cells showing spontaneous synaptic activity were excited by all three of the cardio-respiratory stimuli that caused reflex bradycardia: peripheral chemoreceptor, arterial baroreceptor and nasotrigeminal receptors. Every active cell ($n = 10/10$ tested) responded to each reflex stimulus applied, consistent with their designation as cardiac ganglion principal neurones (see Fig. 5) and indicating a convergence of these vagally mediated reflexes through single ganglion cells (as opposed to each of these vagal reflexes acting though its own segregated population of principal cells). In marked contrast, none of the quiescent cells ($n = 14/14$ tested) showed any response to cardio-respiratory reflex activations.

Peripheral chemoreceptor stimulation by intra-arterial injection of cyanide (30–60 μg), evoked a bradycardia lasting several seconds, with an increase in the frequency and amplitude of phrenic nerve bursts (Paton & Kasparov, 1999). Concurrently there was a strong increase in synaptic activity ($n = 10/10$ cells tested, with a maximum instantaneous EPSP frequency of 65 ± 7 Hz ($n = 6$)) and action potential discharge of the cardiac ganglion cells, which was still modulated by the phase of the respiratory cycle (Fig. 5*A*). However, the EPSPs/action potential discharge now continued into the late expiratory period as well as the postinspiratory phase (e.g. Fig. 7*B*).

Brief ramp increases in perfusion pressure were used to stimulate the arterial baroreceptors. These stimuli elicited a bradycardia that was immediately preceded and accompanied by a rapid volley of action potentials and/or

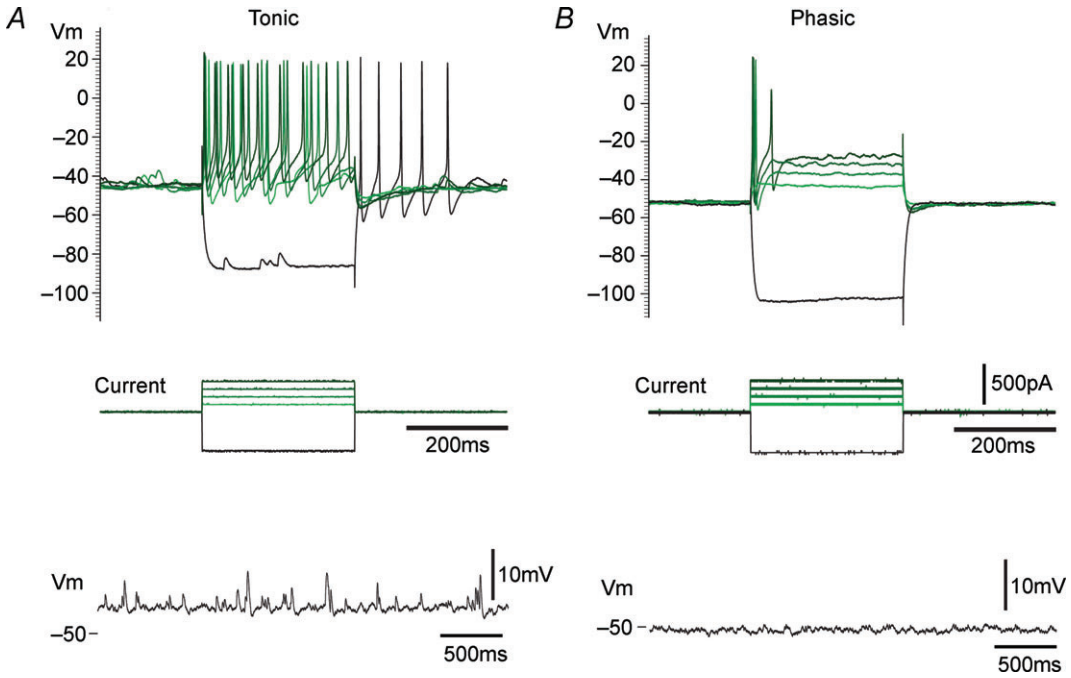

Figure 4. The cardiac ganglion principal cells have distinct intrinsic properties
The cardiac ganglion neurones displayed either tonic (*A*) or phasic (*B*) patterns of discharge in response to injection of depolarising current pulses. The tonic pattern of firing (*A*) was seen exclusively in the spontaneously active principal cells and was never seen in the quiescent cells (representative traces of spontaneous activity shown below – note only the tonic cell shows clear excitatory synaptic potentials). The quiescent cells in contrast showed a phasic pattern of firing with typically only one or at most two spikes being fired in response to depolarising current injection.

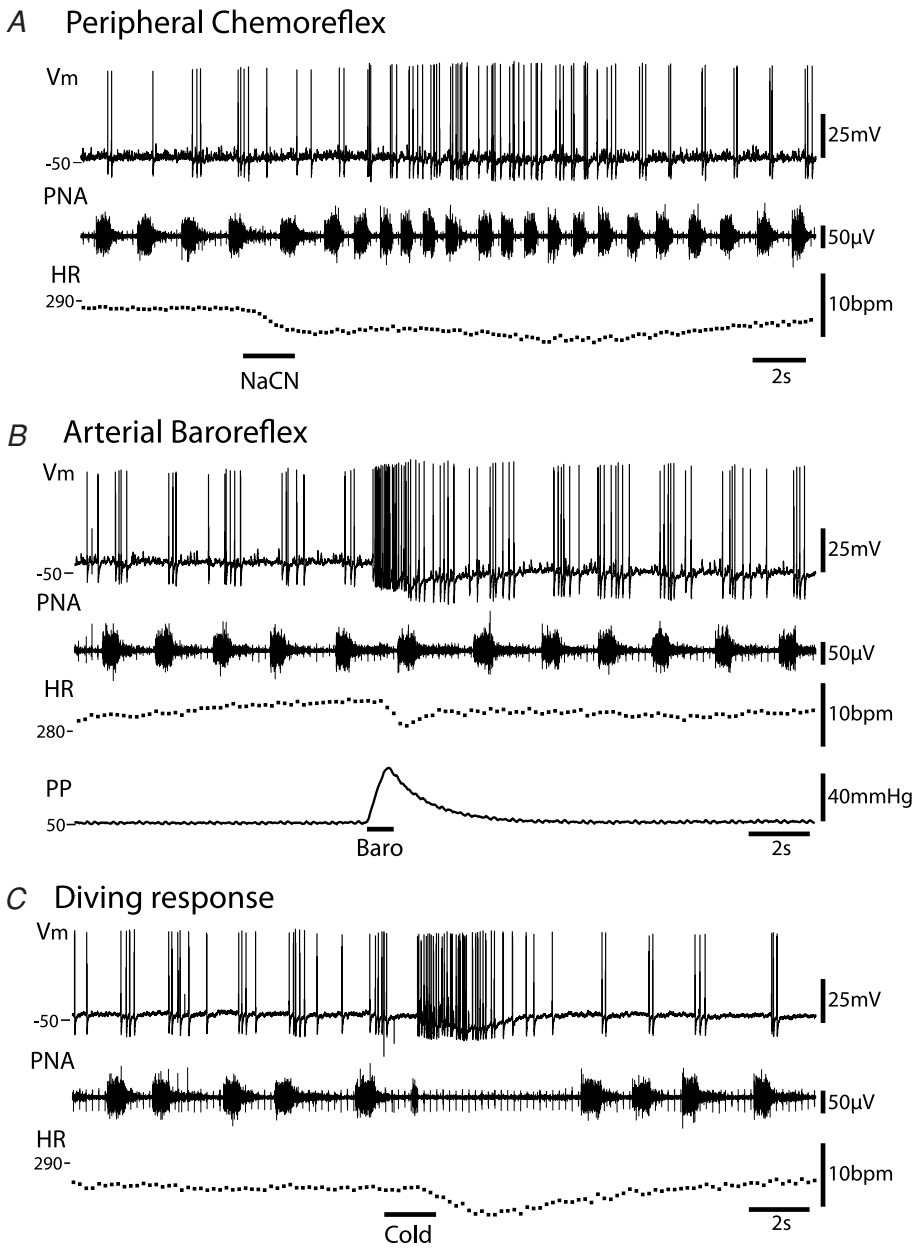

Figure 5. Functional responses of cardiac vagal ganglion principal cells to cardio-respiratory afferent stimulation

All responses shown were obtained from the same neurone. *A*, activation of the peripheral chemoreflex (NaCN 0.03% I.A.) triggered an increase in the discharge frequency of the principal cell along with the tachypnoea. The pattern of action potential discharge was also altered with a spread of firing into the expiratory phase. Both the increase in firing rate and the phase spread recovered as the respiratory response to the chemoreflex activation subsided. *B*, ramp increases in perfusion pressure evoked a barrage of action potential discharge in principal cells which preceded the fall in heart rate. This increase in firing was seen irrespective of the respiratory phase; in this example the discharge is seen to occur predominantly in expiration. Also noteworthy was the summation of the AHPs seen during the activation which caused progressive membrane hyperpolarisation. *C*, the diving response was evoked by the application of cold saline to the snout. This stimulation produced a robust discharge of action potentials from the principal cell. This burst commenced with the onset of the transient apnoea. As with the baroreflex activation, the principal cell was again seen to hyperpolarise during the response. Abbreviations: V_m – membrane potential; PNA – phrenic nerve activity; HR – heart rate; PP – perfusion pressure. (Note the monopolar phrenic nerve recording also includes the ECG signal.)

EPSPs in the ganglion cell (Fig. 5*B*, $n = 7/7$). The rapid synaptic activity following baroreceptor stimulation overrode the resting respiratory modulation, producing action potential firing throughout the respiratory cycle (Fig. 5*B*). These bursts of synaptic activity were only triggered once the perfusion pressure had risen beyond a pressure threshold (25 ± 4 mmHg above the basal perfusion pressure of 70 ± 6 mmHg, $n = 7$, Fig. 6) as has been previously described for both heart rate and cardiac vagal branch discharge (Simms *et al.* 2007). The instantaneous frequency of EPSP discharge above this threshold level was then proportionate to the perfusion pressure and peaked at 55 ± 8 Hz (for ramps to 68 ± 12 mmHg above basal pressure). The EPSP instantaneous frequency followed a similar temporal profile to the perfusion pressure change.

Application of cold Ringer's solution to the snout produced a transient apnoea and a bradycardia – a characteristic diving response. This was associated with a strong barrage of action potentials or EPSPs in the ganglion cell ($n = 2/2$ tested, Fig. 5*C*). When the respiratory cycle resumed, the discharge pattern of these neurones returned to its normal postinspiratory pattern (Fig. 5*C*).

The EPSPs underlying these reflex action potential responses were revealed by passing hyperpolarising current (e.g. Figs 6 and 7). Although there was some temporal summation of EPSPs observed with strong afferent stimulation (seen in Figs 6 and 7) this did not appear to increase the likelihood of EPSPs reaching threshold. At resting membrane potential, even cells that normally showed few subthreshold EPSPs (i.e. had a secure synaptic input) had a higher proportion of EPSPs that failed to evoke action potentials during strong reflex stimulation (Fig. 7). Several possible mechanisms were observed that may account for this effect including frequency-dependent synaptic depression, summation of the after-hyperpolarisations (AHPs), and limits on temporal summation imposed by the refractory period of action potential discharge in the single active preganglionic (see below).

When particularly strong reflex stimuli (baroreceptor, diving) triggered rapid trains of action potentials there was a hyperpolarising shift in baseline membrane potential (Fig. 5*B* and *C*). No hyperpolarising shift occurred if action potential discharge was prevented by the injection of steady hyperpolarising current (Fig. 6). The membrane potential shift was likely due to summating AHPs.

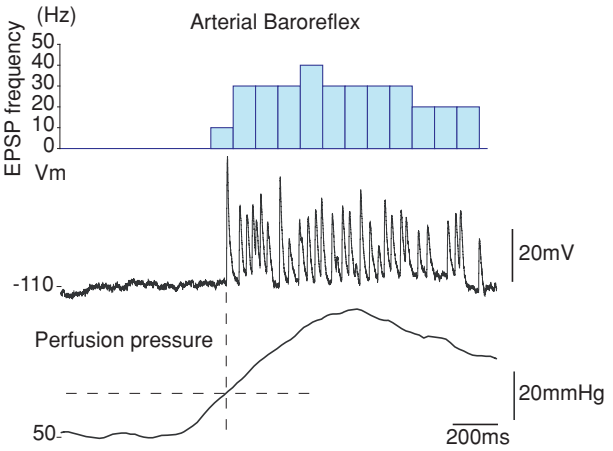

Figure 6. Baroreflex excitation of cardiac vagal ganglion principal cells
Increasing the perfusion pressure (by increasing perfusate flow) produced a train of EPSPs (revealed by injection of hyperpolarising current) that underlay the spike discharge of principal cells (seen in Fig. 5*B*). These EPSPs were only triggered once the pressure passed a threshold level of ~20 mmHg above basal perfusion pressure (dotted lines). The frequency of discharge mirrored the rise in pressure to reach a maximum frequency of 40 Hz at the peak of the pressure response. The EPSPs were seen to temporally summate during the peak of the response although this was counterbalanced by the diminished amplitude of the closely consecutive synaptic events. This suggests the potential for intricate synaptic integration within the principal cells.

Vagal stimulation evokes EPSPs in principal neurones

Principal neurones. All of the neurones with ongoing synaptic activity that were tested showed vagal stimulation-evoked synaptic potentials that could drive action potential discharge ($n = 6/6$, Fig. 8*A*). In addition, three previously silent cells that had minimal ongoing synaptic activity showed vagal-evoked EPSPs. In all of these vagally activated neurones the injection of hyperpolarising current revealed the underlying EPSPs, which had a stable latency (range 21–65 ms, mean 33.7 ± 5.1 ms, $n = 9$) with a relatively small jitter (349 ± 86 μs, $n = 6$, SD, measured over 25–50 vagal stimuli), and estimated conduction velocity ranging from 0.35 to 1.15 m s^{-1} compatible with a monosynaptic input (Fig. 8*B*). The waveform of the evoked EPSP was strikingly similar to the spontaneous EPSPs (Fig. 8*C*). As the intensity of the vagal stimulus was gradually reduced, a point was reached where the EPSP failed, apparently in all-or-nothing fashion.

In two of these six active cells, electrical stimulation evoked a double synaptic event. The first was found at a latency of 20–25 ms and the later EPSP at a latency of 60–70 ms (Fig. 9). Superimposition of successive traces showed that the second synaptic event had more jitter and more frequent failures of synaptic transmission (Fig. 9*A*). Notably the amplitude and waveform of this second EPSP was otherwise very similar to the earlier event. The early event could be dissociated from the second by decreasing the stimulus intensity. Furthermore, the amplitude of this early EPSP was significantly attenuated by the occurrence of preceding spontaneous EPSPs (suggesting that it exhibited frequency-dependent depression, see below)

unlike the later EPSP. From these data we hypothesise that these EPSPs may reflect convergent vagal inputs onto a single cardiac ganglion cell and that only one of these inputs is from a vagal preganglionic neurone with spontaneous activity (see below).

Following each vagal stimulus-evoked EPSP (single or double) there was a pause in the occurrence of spontaneous EPSPs lasting 116 ± 14 ms from the earliest evoked EPSP ($n = 5$, Fig. 9*B*). This is likely to be due to the relative refractoriness of the preganglionic neurone following stimulus induced antidromic invasion (the vagus nerve was intact in all of these experiments; it is worth noting, however, that these vagal stimuli (0.5–1 Hz) did not reset or entrain the respiratory cycle).

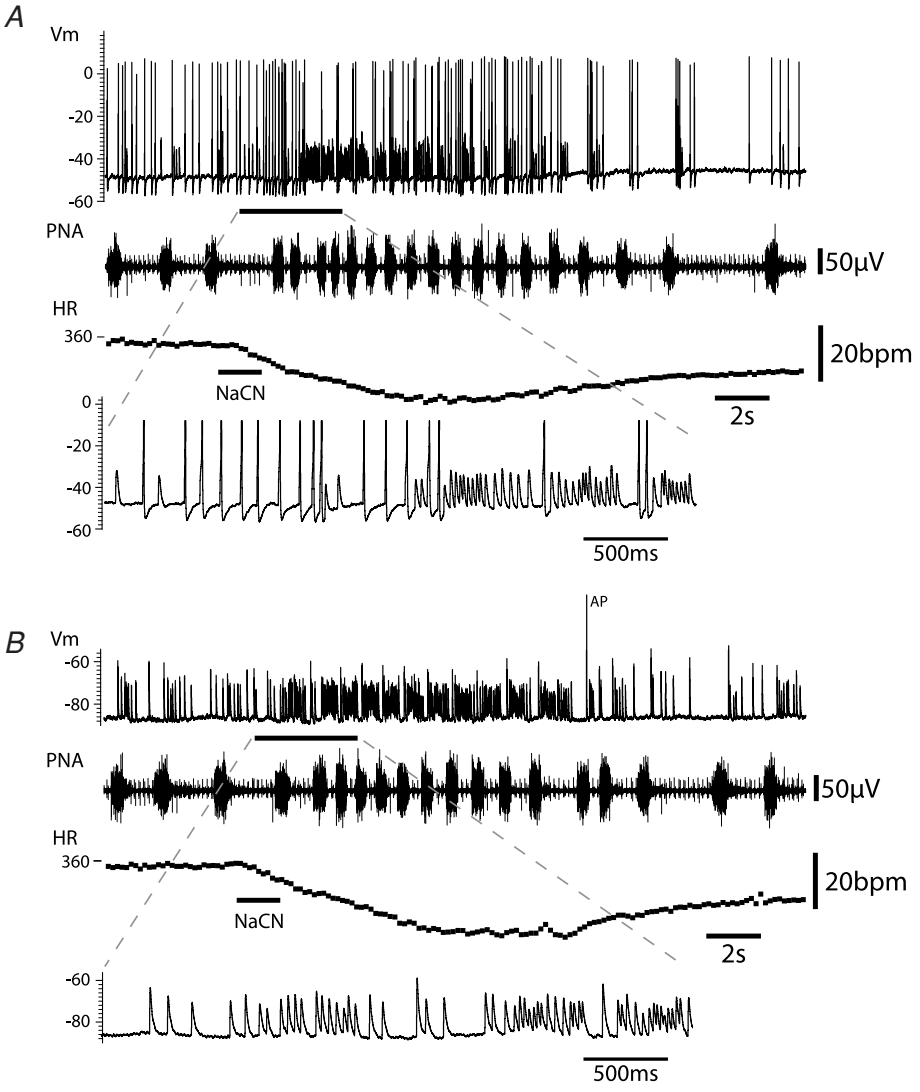

Figure 7. Peripheral chemoreflex-evoked EPSP drive to principal cells
A, activation of the peripheral chemoreflex (I.A. NaCN) evoked an initial strong increase in action potential discharge and also a clear increase in the frequency of large EPSPs. However during much of the response there was an excess of subthreshold EPSPs relative to action potentials, indicating a gearing of ganglionic throughput from pre- to postganglionic neurones. *B*, with the cell hyperpolarised (by current injection) to prevent action potential discharge, activation of the peripheral chemoreflex clearly evoked a striking increase in the frequency of EPSPs. These EPSPs were seen to occur across much of the respiratory cycle with only a brief pause during early inspiration suggesting strong gating of the central drive from the cardiac vagal preganglionic neurones during this phase of the cycle. The first EPSP in the burst was often the largest and this often coincided with the phase when action potential discharge was evident under basal conditions (in the immediate postinspiratory phase). There was weak temporal summation of the EPSPs during this stimulus (as shown on the expanded time base) offset again by the diminishing amplitude of the synaptic events during high frequency bursts. (Note the monopolar phrenic nerve recording also includes the ECG signal.)

Quiescent cells. Vagal stimulation never evoked EPSPs in the quiescent cells ($n = 6/6$ tested). However, in one of these cells a putative antidromic spike was evoked by vagal stimulation. The evoked spike was not preceded by a discernable synaptic event and had a fixed latency (unlike synaptically evoked firing), and no underlying EPSP was revealed by hyperpolarisation (data not shown). This may therefore have been a vagal afferent neurone with a sensory function, as described for cells in the guinea pig cardiac ganglia *in vitro* (Edwards *et al.* 1995) and also demonstrated by retrograde labelling from the nodose ganglion in the rat (Cheng *et al.* 1997).

Spontaneous synaptic activity is driven by single preganglionic neurones

When the time series of all spontaneous synaptic events for each principal cell were plotted as autocorrelation histograms (autocorrelograms), a central valley was always apparent, with zero counts surrounding the trigger event (Fig. 10*A*; 10/10 neurones, mean width of absolute refractory period 22.5 ± 5.7 ms). This pattern demonstrates that the spontaneous inputs came from a single active presynaptic source, with relative and absolute refractory periods (cf. Bratton *et al.* 2010). Note that these refractory periods originate in the preganglionic neurone (no refractory period applies to postsynaptic potentials). To demonstrate the veracity of this test, the true autocorrelogram (Fig. 10*A*) may be contrasted with a second autocorrelogram that was constructed from the same data set, retaining the same mean frequency but manipulated to simulate two separate, independent inputs (Fig. 10*B*, details in Methods): the central gap disappears when two or more inputs are active. The central gap was retained by all studied neurones, even when synaptic activity was driven strongly by reflexes where there was an absolute minimum interval between consecutive EPSPs of 4–5 ms, and a corresponding central gap in the autocorrelogram. This matches the minimum interval observed between consecutive

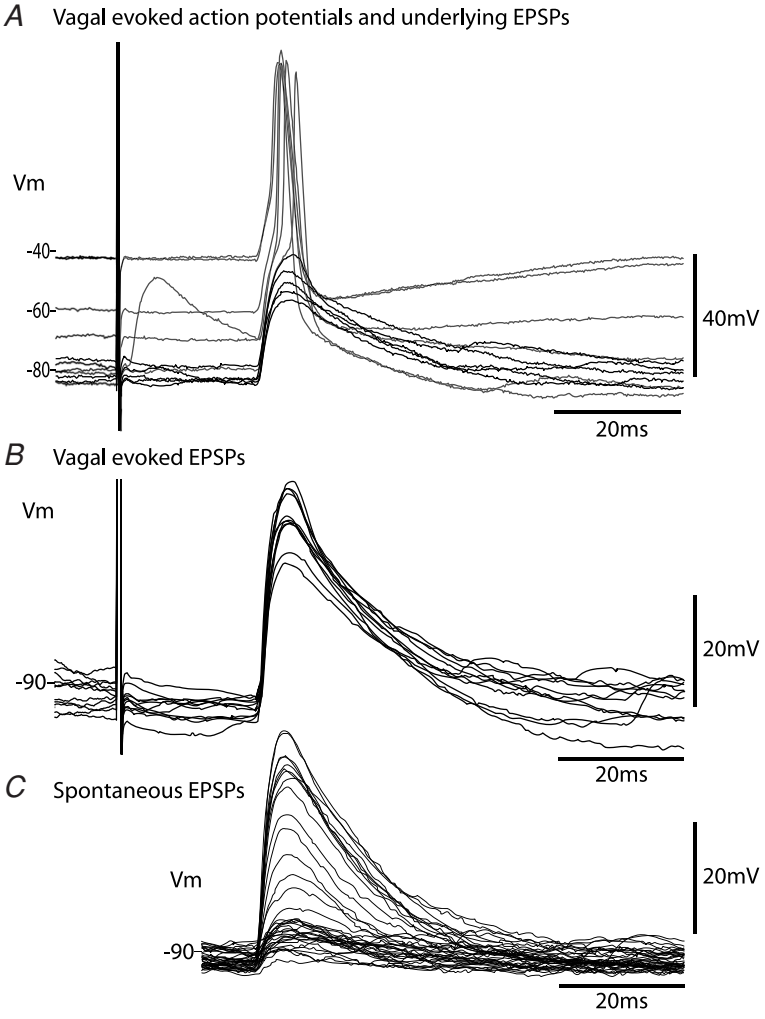

Figure 8. Vagally evoked and spontaneous EPSPs in cardiac vagal ganglion principal cells
A, stimulation of the cervical vagus nerve with a bipolar electrode (4.75 V, 1 ms) reliably evoked action potential discharge in the principal cell at rest. Progressive hyperpolarisation (by injecting current) to potentials below –70 mV prevented action potential discharge and revealed the underlying postsynaptic potential with a latency of 22 ms and a jitter of 140 μs (SD of latency over 50 sweeps). *B*, overlaid consecutive evoked EPSPs ($n = 10$) showing the constant latency, lack of failures and small variation in amplitude. Note only a single event was evoked in this principal cell. *C*, comparison with spontaneous EPSPs in the same cell, which show a similar waveform to the evoked EPSPs. The spontaneous events have a broader spectrum of amplitudes, but even the smaller events follow the same time course. (~2.1 Hz spontaneous event rate.)

action potentials of cardiac vagal preganglionic neurones in the rat nucleus ambiguus *in vivo* (Toader *et al.* 2008).

Frequency-dependent depression of EPSP amplitudes

In principal cells, when action potential discharge was prevented by hyperpolarising current, it could be seen that the amplitudes of successive EPSPs varied strikingly (as illustrated in Fig. 2*B* and *C*). This was despite their apparently originating from a single preganglionic source (see above) and therefore via the same synapse. To test whether this could be due to frequency-dependent synaptic depression (as described *in vitro*; Seabrook *et al.* 1990; Selyanko & Skok, 1992; Rimmer & Harper, 2006), EPSP amplitudes were plotted against the interval since the preceding EPSP (Fig. 11). A significant positive correlation between EPSP amplitude and the interval since the previous EPSP, consistent with frequency-dependent synaptic depression, was evident in 8/10 cases tested (and a similar non-significant trend was seen in the remaining two cells).

Discussion

It has hitherto been technically challenging to make direct intracellular studies of the synaptic transmission processes through the cardiac ganglion under naturalistic conditions. We have taken advantage of the WHBP approach to make stable intracellular recordings from cardiac vagal ganglion neurones on the surface of the beating atrium while they are still functionally connected to their natural inputs (central and peripheral). This has led to novel insights into how the principal neurones of the cardiac ganglion receive ongoing and reflex synaptic drive from the brainstem, and how they process and integrate these neural signals before relaying them as vagal tone to the heart.

The key observations are, first, that within the cardiac ganglion only a proportion of neurones were vagal postganglionic motoneurones (the principal cells, 41%). These showed ongoing action potentials and/or EPSPs, the occurrence of which was strongly modulated by the respiratory cycle, consistent with their carrying vagal tone to the heart. Second, these principal cells

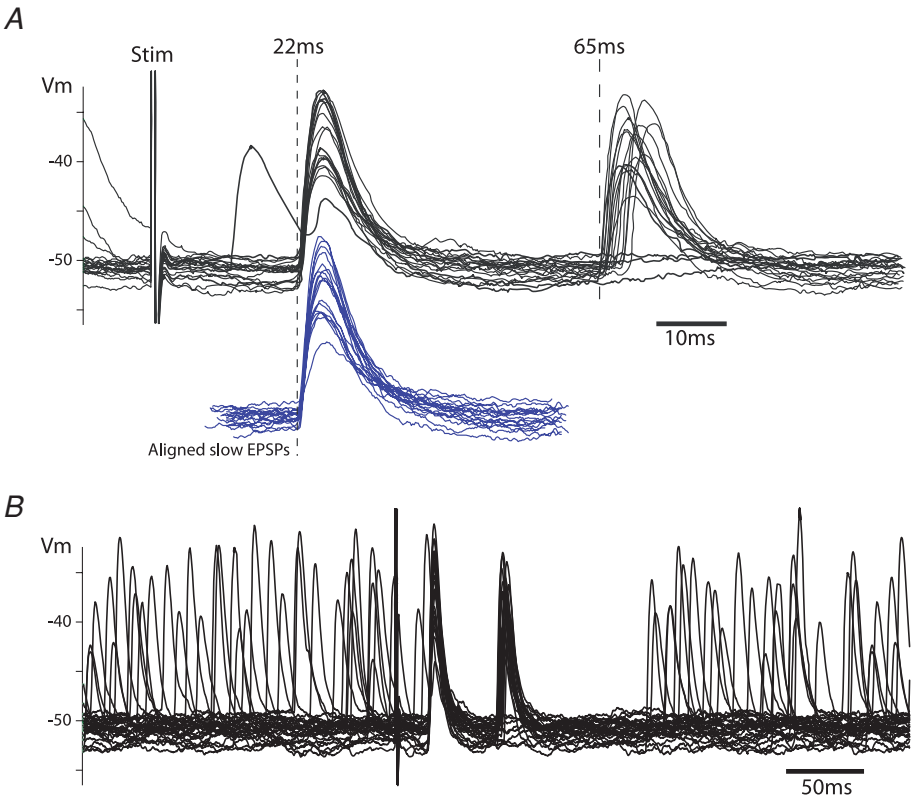

Figure 9. Vagal stimulus-evoked double EPSPs in cardiac vagal ganglion principal cells
A, stimulation of the cervical vagus nerve with a bipolar electrode evoked EPSPs at latencies of 22 ms and 65 ms (corresponding to conduction velocities of 1 m s^{-1} and 0.3 m s^{-1}, respectively). The second EPSP had a higher failure rate and substantially more jitter in its latency than the earlier EPSP. However, by aligning the onset of the second EPSP it could be seen that the waveform and amplitude was remarkably similar to the early EPSP (shown below in blue). *B*, on a slower time base the refractory period after the vagal stimulation evoked EPSPs is seen as lasting 120 ms, during which time spontaneous events were suppressed.

were excited by all of the tested cardio-respiratory reflexes (arterial baroreceptor, peripheral chemoreceptor, diving), indicating a convergence of these reflexes through individual ganglion cells. Third, we show that synaptic transmission through the ganglion is not always secure and in most principal cells there is a less than 1:1 correspondence between incoming EPSPs and action potential discharge, especially under conditions of strong reflex activation. Fourth, action potentials arise from unitary EPSPs. Fifth, principal neurones appear to have a single active preganglionic synaptic input that accounts for their spontaneous and reflex-evoked discharge. Sixth, the EPSPs from this preganglionic input show frequency-dependent depression, within the physiological range of discharge frequencies, which (along with the intrinsic properties of the principal cells) may account for the loss of transmission efficacy seen during strong afferent stimulation. Finally, vagal stimulation can demonstrate the presence of functionally silent synaptic inputs to a subset of these principal neurones.

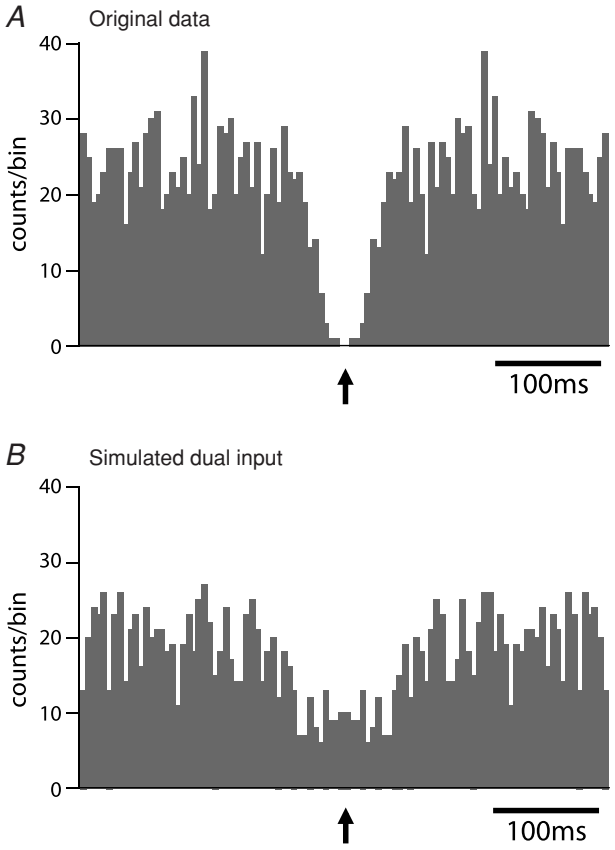

Figure 10. Spontaneous EPSPs in cardiac vagal ganglion principal cells come from a single vagal preganglionic source
A, with the cell hyperpolarised for 2 min to prevent action potential discharge the EPSPs were discriminated from the first derivative of the voltage trace and plotted as an autocorrelogram (bin width 5 ms). This showed a distinctive central valley feature with an absolute period of synaptic silence of 10 ms and a relative quiescent period (half valley width) of around 150 ms. This pattern of autocorrelogram strongly suggests that the spontaneous EPSPs were originating form a single active preganglionic neurone and the valley is a consequence of the absolute and relative refractory periods of the parasympathetic preganglionic neurone. *B*, to illustrate the effect of having two active independent preganglionic neurones, the data from the first minute and the second minute of the recording in *A* were overlaid on a single time series that was then stretched twofold in the time domain. This was used to represent an equivalent data set but from two independent preganglionic inputs. As can be seen the central valley feature is lost.

Together, these findings indicate that the convergence between the different cardio-respiratory afferent evoked cardiac vagal reflexes occurs at, or before, the parasympathetic preganglionic neuron. Our observation of a less than 1:1 ratio of EPSP:action potential discharge in the principal cells shows that the cardiac ganglion can modulate the gain of the vagal drive that it transmits to the heart. This appears not to be the product of spatial or temporal summation or fast inhibitory neurotransmission, but rather of frequency-dependent synaptic depression, refractoriness of preganglionic firing and summation of slow AHPs. In addition it is likely that other factors both intrinsic to the principal cells and local to the ganglion will account for the variable gain of transmission seen through individual ganglion cells in this study.

Use of WHBP to study cardiac ganglion neurotransmission

There are both technical advantages and limitations inherent in our initial study. On the positive side, the preparation allows reliable stabilisation of the cardiac ganglia on the atrial surface while the heart is still beating. This can be achieved in an *in vivo*-like situation as the preparation is not dependent upon the cardiac output for its viability and there is a bloodless recording field. Importantly the WHBP is un-anaesthetised and displays cardiac vagal 'tone' with respiratory sinus arrhythmia (Paton, 1996; Simms *et al.* 2007). This indicates that the brainstem processes generating vagal tone, its respiratory modulation and the pathways that transmit it via the cardiac ganglia to the heart are all intact. As further evidence of the physiological integrity of the preparation, vagal synaptic drive was activated promptly and vigorously by three reflex stimuli: arterial baroreceptors, peripheral chemoreceptors and diving response.

One difference of the WHBP with ventricles detached (as used herein) from conditions *in vivo* is the lack of an arterial pulse pressure, which via arterial baroreflex inputs may have altered the pulsatile grouping of vagal preganglionic action potentials. This delivery of pulse modulated packets of EPSPs could influence the synaptic integration at the ganglion *in vivo* (McAllen & Spyer, 1978; Rentero *et al.* 2002). A second confound

is that the atria were partly separated from the ventricles, potentially disconnecting some intra-cardiac reflex pathways (Armour, 2008) that may be relevant to the absence of activity seen in the local circuit ganglion cells. Other relevant factors here may be the relative lack of atrial wall motion in the stabilised area, and the loss of chest wall movement plus the open chest wall and pericardium, which may all contribute to a diminished local sensory input. It is also worth noting that there will be a dilution of circulating factors such as hormones in the perfusate that may normally modulate ganglionic excitability *in vivo*.

The preparation is subject to neuromuscular blockade to permit stable intracellular recordings and although some competitive muscle relaxants (e.g. pancuronium and gallamine) are known to affect ganglionic transmission, vecuronium was employed here as it was developed specifically to exert minimal vagolytic actions (Bowman *et al.* 1988). The vigorous vagal control of the heart seen in the preparation (in terms of tonic rate control, presence of respiratory sinus arrhythmia and cardio-respiratory reflex evoked bradycardias; see also Paton, 1996; Paton & Kasparov, 1999; Pickering *et al.* 2002; Pickering & Paton, 2006) support this selectivity of vecuronium for the muscle nicotinic receptor, and it would seem unlikely to be exerting a significant effect on cardiac ganglionic transmission. Additionally the recordings were made at a temperature of 32°C (compared to the more typical 35–37°C used *in vitro* for intracellular recordings). This lower temperature will have slowed the kinetics of synaptic transmission and action potential conduction velocity to an extent; however, we and others have made many cellular recording studies using the WHBP in a variety of brain regions with both extracellular and patch recordings and have found results that were directly comparable to those found *in vivo* or in reduced slice preparations. In sum, these drawbacks of the WHBP for this type of experiment are relatively minor, especially since there are no alternative preparations that permit intracellular recordings with intact central pathways.

Functional phenotyping of ganglion cells

Our finding that only a minority of the cardiac ganglion cells are principal neurones (41%) is in agreement with previous *in vitro* studies that showed a similar proportion of cells to receive vagal inputs in the guinea pig (Edwards *et al.* 1995) and inferred from local interconnective stimulation experiments in the rat cardiac ganglion (Selyanko & Skok, 1992). These neurones exhibited a distinct pattern of synaptic inputs consistent with that expected for vagal tone with maximum activity in

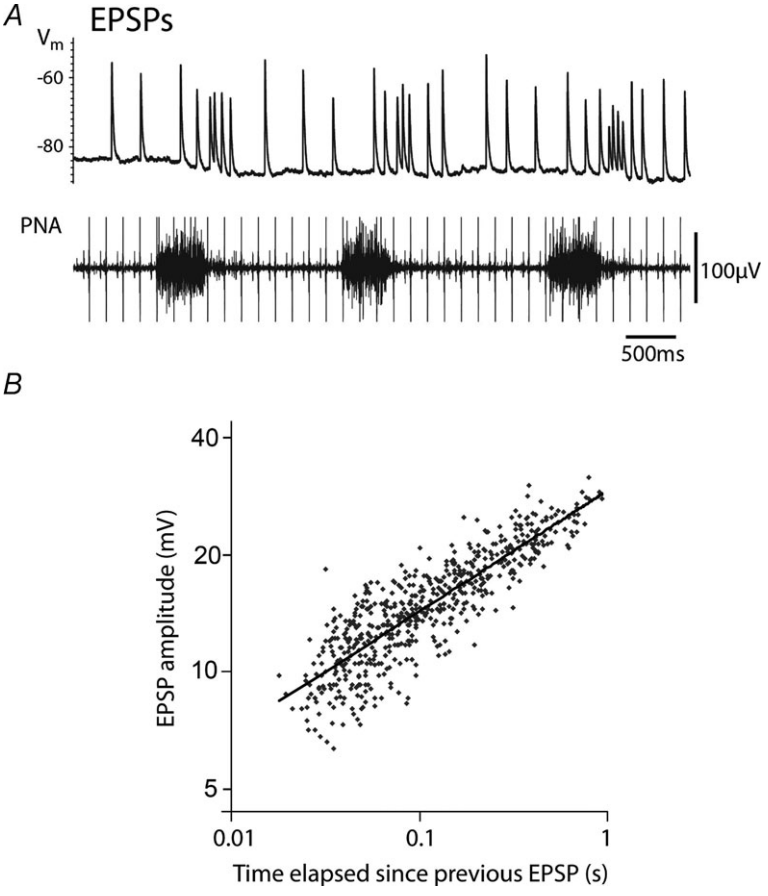

Figure 11. Frequency-dependent depression of EPSP amplitude in cardiac vagal ganglion principal cells
A, recording of a principal cell with spontaneous EPSPs showing the increased frequency of events in the postinspiratory phase (membrane potential hyperpolarised by current injection to prevent action potential discharge). It was also notable that as the inter-EPSP interval shortened so the amplitude of each EPSP appeared to be attenuated. (Note the monopolar phrenic nerve recording also includes the ECG signal.) *B*, a log-log plot of EPSP amplitude against time since the previous EPSP revealed a striking correlation, indicating that synaptic transmission at this site shows frequency-dependent depression.

post-inspiration and a minimum in early inspiration. This matches that measured in anaesthetised cats (McAllen & Spyer, 1978) and dogs (Hayano *et al.* 1996) and that inferred from indirect measures in man (Sin *et al.* 2010).

We suggest that the remainder of recorded neurones are likely to be interneurones and perhaps local or centrally projecting sensory neurones. Intriguingly, these were invariably silent in our preparations and had a low level of synaptic input (unlike the recordings of Edwards (1995)), raising the question of what their effective stimulus was. They were not activated by any of the cardio-respiratory reflex manoeuvres; nor did we find any that were synaptically excited by vagal stimulation (although one was antidromically activated). Therefore, the question of whether and how they act as 'a cardiac brain' to modulate ganglion function in health and disease remains an intriguing issue (Armour *et al.* 1998; Arora *et al.* 2003; Armour, 2008). As mentioned previously, the recording conditions employed in our study may have exposed these neurones to an environment that is mechanically and biochemically different from that found in working cardiac muscle tissues (and hence arrested their discharge). In future experiments it will be appropriate to attempt to stimulate these cells by application of agents known to trigger cardiac afferent reflexes such as bradykinin, adenosine and capsaicin or indeed ischaemia.

The principal neurones were distinguishable from the other ganglion cells on the basis of their intrinsic properties (as well as synaptic drives). The principal cells fired tonically in response to depolarising current pulses whereas the other neurones had phasic patterns of firing, which is reminiscent of the classification of guinea pig and rat cardiac vagal neurones *in vitro* (Selyanko, 1992; Selyanko & Skok, 1992; Edwards *et al.* 1995; Hardwick *et al.* 2009). The intrinsic properties of the principal cells are relevant to their functional role of processing the vagal drive to the heart. Specifically, the prominent AHPs of the principal cells may act to restrict spike discharge by summing to produce the hyperpolarisation observed during intense cardio-respiratory afferent stimulation (Fig. 5*B* and *C*).

Functional organisation of efferent vagal drive to principal neurones

All of the principal ganglion cells responded to all of the tested cardio-respiratory afferents with barrages of EPSPs and the discharge of action potentials. This indicates that there is convergence of these different vagal reflexes onto single cardiac postganglionic neurones. The observation that the spontaneously active synaptic events originate from a single input, based on autocorrelograms, indicates that the convergence of reflex arcs occurs at the level of the parasympathetic preganglionic neurones in the medulla. These findings are in broad agreement with previous anterograde tracing studies (Cheng, 1997, 2004).

Interestingly, our vagal stimulation experiments may have also shown evidence for silent synaptic inputs. In two of the principal cells a double synaptic response was observed (like Seabrook *et al.* 1990) and the amplitude of the second EPSP, unlike the first, appeared to be little affected by the preceding discharge of spontaneous EPSPs. In addition the later EPSP did fail more frequently and had a higher threshold for activation, suggesting that it was an independent event and was functionally 'silent'. A further three principal neurones with synaptic inputs from the vagus nerve showed no ongoing vagal tone, presumably also reflecting the fact that their preganglionic neurones had no spontaneous discharge. Such silent preganglionic neurones have been encountered frequently in the nucleus ambiguus of anaesthetised cats (McAllen & Spyer, 1978) and rats (Rentero *et al.* 2002) or alternatively these synaptic inputs may be from the dorsal vagal motor nucleus (Jones, 2001).

One possible alternative explanation for the presence of the double EPSP is that the later event may be caused by activation of the intact vagal afferent fibres by the electrical stimulus to evoke a reflex arc response transmitted via the brainstem and out on the vagal preganglionic fibres. We think this unlikely as the second EPSP was only seen in a minority of principal cells (2/9), its latency is relatively short for such a reflex loop and it falls in a time window when the preganglionic neurones would be relatively refractory following the earlier EPSP. Selective stimulation either focally in the brainstem or of de-afferented vagi will be required to definitively distinguish between these possibilities.

Vagal synaptic transmission through principal neurones

It is apparent from our data that synaptic transmission at the cardiac vagal ganglionic synapse *in vivo* does not behave as a 1:1 relay, at least in the sinoatrial ganglion. Although in some cells the vagal EPSPs were often suprathreshold, and required strong hyperpolarisation to potentials below –80 mV to reveal the underlying EPSPs, the events demonstrated considerable variability in amplitude. Many subthreshold EPSPs were observed, even during strong cardio-respiratory reflex activation, and indeed these were commoner at higher preganglionic firing frequencies. This is likely to relate to the observed frequency-dependent synaptic depression, also previously noted *in vitro* (Seabrook *et al.* 1990; Selyanko & Skok, 1992; Rimmer & Harper, 2006), which overpowers the potential for temporal summation of EPSPs. Physiologically, the frequency-dependent synaptic depression will act to limit

the rate of onward transmission of vagal impulses to the heart, particularly during intense barrages such as in the postinspiratory period. As noted earlier, there is also likely to be a role for the postsynaptic integrative properties such as the AHP in regulating synaptic throughput. This synapse is therefore a locus where the efficiency of transmission may be modulated by extrinsic or intrinsic factors.

Previous studies on the vagal inputs to cardiac ganglion cells *in vitro* have noted the presence and properties of 'strong' or 'dominant' synapses (Seabrook *et al.* 1990; Selyanko & Skok, 1992; Rimmer & Harper, 2006). This type of input to autonomic ganglion cells is characterised by a high safety factor, triggering action potentials that are difficult to block even with strong hyperpolarising current (McLachlan & Meckler, 1989; Selyanko & Skok, 1992; Bratton *et al.* 2010). Following those action potentials, the tail of the large EPSP persists and generally causes an afterdepolarisation, or at least offsets any early after-hyperpolarisation (McLachlan & Meckler, 1989; Seabrook *et al.* 1990; Selyanko & Skok, 1992; McLachlan *et al.* 1997; Ireland *et al.* 1999; Rimmer & Harper, 2006). Both the safety factor and the afterdepolarisation decrease with repetition in a frequency-dependent manner (Selyanko & Skok, 1992; Rimmer & Harper, 2006). Rimmer & Harper (2006) classified synaptic inputs to rat cardiac ganglion cells as 'strong', 'secure' (i.e. generally suprathreshold) or 'weak' (subthreshold), and between one-third and one-half of their sample received 'strong' synaptic inputs, with most of the remainder receiving 'secure' inputs.

In the present study of 13 ganglion cells with vagal inputs ($n = 9$ electrically evoked), we encountered one clear example of a dominant ('strong') synaptic input with the remainder being either variably secure or weak. It may be significant that the cell with the strong input showed no ongoing activity. The relative scarcity of strong inputs here compared with previous *in vitro* studies deserves comment. First, this was a small sample of cells, and either chance or some unrecognised bias could have mitigated against us recording cells with dominant inputs. Second, a key difference of the present study is that ongoing synaptic activity (typically ~4Hz Hz) would have caused frequency-dependent depression of transmitter release, especially since the EPSPs are grouped in bursts by respiratory modulation. This compares with electrical vagal stimulation *in vitro* typically at 1 Hz or less. It is conceivable that the observed frequency-dependent synaptic depression may have changed some 'strong' synapses to 'secure', and 'secure' synapses to 'weak' with short-term plasticity. Our observations demonstrate that cardiac vagal ganglionic transmission is not a rigid 1:1 process, leaving ample scope for physiological and pathophysiological factors to modulate the vagal tone transmitted on to the heart.

Implications of cardiac ganglion gating of vagal neurotransmission

We conclude that there is considerable reserve synaptic capacity in the cardiac ganglion, represented by the occurrence of subthreshold EPSPs and also the presence of a population of silent synapses. As has been proposed for sympathetic vasomotor ganglionic transmission (Bratton *et al.* 2010), a minor shift in ganglion cell threshold or resting potential could substantially affect the proportion of preganglionic inputs that trigger postganglionic action potentials. Similarly modulation of the frequency-dependent synaptic depression or the magnitude of the AHP will also dramatically sculpt the ganglionic throughput. Interestingly several studies have reported changes in the integrative properties of cardiac ganglion neurones in cardiovascular disease models (Hardwick *et al.* 2008, 2009). These findings mark the cardiac ganglion as a key player in determining the level of vagal tone, balancing local and central factors. This becomes particularly important when we consider that the loss of vagal tone to the heart is found in a number of cardiovascular diseases such as heart failure, after myocardial infarction, in hypertension and diabetes, and is an independent predictor of mortality and morbidity (La Rovere *et al.* 1998, 2003; Nolan *et al.* 1998). Alterations in the mechanisms that gate synaptic transmission either pre- or postsynaptically could account for the loss of vagal tone at the level of the vagal ganglion synapse as has been reported in experimental heart failure (Bibevski & Dunlap, 1999; Arora *et al.* 2003) and hypertension (Heaton *et al.* 2007). Our findings indicate that therapeutic interventions targeted at the cardiac ganglion (e.g. Mohan *et al.* 2002; Bibevski & Dunlap, 2004) could restore vagal tone by opening the synaptic gate to recruit the reserve vagal capacity.

References

Armour JA (2008). Potential clinical relevance of the 'little brain' on the mammalian heart. *Exp Physiol* **93**, 165–176.

Armour JA, Collier K, Kember G & Ardell JL (1998). Differential selectivity of cardiac neurons in separate intrathoracic autonomic ganglia. *Am J Physiol Regul Integr Comp Physiol* **274**, R939–949.

Arora RC, Cardinal R, Smith FM, Ardell JL, Dell'Italia LJ & Armour JA (2003). Intrinsic cardiac nervous system in tachycardia induced heart failure. *Am J Physiol Regul Integr Comp Physiol* **285**, R1212–1223.

Bibevski S & Dunlap ME (1999). Ganglionic mechanisms contribute to diminished vagal control in heart failure. *Circulation* **99**, 2958–2963.

Bibevski S & Dunlap ME (2004). Prevention of diminished parasympathetic control of the heart in experimental heart failure. *Am J Physiol Heart Circ Physiol* **287**, H1780–1785.

Bowman WC, Rodger IW, Houston J, Marshall RJ & McIndewar I (1988). Structure:action relationships among some desacetoxy analogues of pancuronium and vecuronium in the anesthetized cat. *Anesthesiology* **69**, 57–62.

Bratton B, Davies P, Janig W & McAllen R (2010). Ganglionic transmission in a vasomotor pathway studied in vivo. *J Physiol* **588**, 1647–1659.

Cheng Z, Powley TL, Schwaber JS & Doyle FJ 3rd (1997). Vagal afferent innervation of the atria of the rat heart reconstructed with confocal microscopy. *J Comp Neurol* **381**, 1–17.

Cheng Z, Zhang H, Guo SZ, Wurster R & Gozal D (2004). Differential control over postganglionic neurons in rat cardiac ganglia by NA and DmnX neurons: anatomical evidence. *Am J Physiol Regul Integr Comp Physiol* **286**, R625–633.

Edwards FR, Hirst GD, Klemm MF & Steele PA (1995). Different types of ganglion cell in the cardiac plexus of guinea-pigs. *J Physiol* **486**, 453–471.

Hardwick JC, Baran CN, Southerland EM & Ardell JL (2009). Remodeling of the guinea pig intrinsic cardiac plexus with chronic pressure overload. *Am J Physiol Regul Integr Comp Physiol* **297**, R859–866.

Hardwick JC, Southerland EM & Ardell JL (2008). Chronic myocardial infarction induces phenotypic and functional remodeling in the guinea pig cardiac plexus. *Am J Physiol Regul Integr Comp Physiol* **295**, R1926–1933.

Hayano J, Yasuma F, Okada A, Mukai S & Fujinami T (1996). Respiratory sinus arrhythmia. A phenomenon improving pulmonary gas exchange and circulatory efficiency. *Circulation* **94**, 842–847.

Heaton DA, Li D, Almond SC, Dawson TA, Wang L, Channon KM & Paterson DJ (2007). Gene transfer of neuronal nitric oxide synthase into intracardiac ganglia reverses vagal impairment in hypertensive rats. *Hypertension* **49**, 380–388.

Ireland DR, Davies PJ & McLachlan EM (1999). Calcium channel subtypes differ at two types of cholinergic synapse in lumbar sympathetic neurones of guinea-pigs. *J Physiol* **514**, 59–69.

Jones JF (2001). Vagal control of the rat heart. *Exp Physiol* **86**, 797–801.

La Rovere MT, Bigger JT Jr, Marcus FI, Mortara A & Schwartz PJ (1998). Baroreflex sensitivity and heart-rate variability in prediction of total cardiac mortality after myocardial infarction. ATRAMI (Autonomic Tone and Reflexes After Myocardial Infarction) Investigators. *Lancet* **351**, 478–484.

La Rovere MT, Pinna GD, Maestri R, Mortara A, Capomolla S, Febo O, Ferrari R, Franchini M, Gnemmi M, Opasich C, Riccardi PG, Traversi E & Cobelli F (2003). Short-term heart rate variability strongly predicts sudden cardiac death in chronic heart failure patients. *Circulation* **107**, 565–570.

Lichtman JW (1977). The reorganization of synaptic connexions in the rat submandibular ganglion during post-natal development. *J Physiol* **273**, 155–177.

McAllen RM & Spyer KM (1978). Two types of vagal preganglionic motoneurones projecting to the heart and lungs. *J Physiol* **282**, 353–364.

McLachlan EM, Davies PJ, Habler HJ & Jamieson J (1997). On-going and reflex synaptic events in rat superior cervical ganglion cells. *J Physiol* **501**, 165–181.

McLachlan EM & Meckler RL (1989). Characteristics of synaptic input to three classes of sympathetic neurone in the coeliac ganglion of the guinea-pig. *J Physiol* **415**, 109–129.

Melnitchenko LV & Skok VI (1970). Natural electrical activity in mammalian parasympathetic ganglion neurones. *Brain Res* **23**, 277–279.

Mohan RM, Heaton DA, Danson EJ, Krishnan SP, Cai S, Channon KM & Paterson DJ (2002). Neuronal nitric oxide synthase gene transfer promotes cardiac vagal gain of function. *Circ Res* **91**, 1089–1091.

Nolan J, Batin PD, Andrews R, Lindsay SJ, Brooksby P, Mullen M, Baig W, Flapan AD, Cowley A, Prescott RJ, Neilson JM & Fox KA (1998). Prospective study of heart rate variability and mortality in chronic heart failure: results of the United Kingdom heart failure evaluation and assessment of risk trial (UK-heart). *Circulation* **98**, 1510–1516.

Paton JF (1996). A working heart-brainstem preparation of the mouse. *J Neurosci Methods* **65**, 63–68.

Paton JF & Kasparov S (1999). Differential effects of angiotensin II on cardiorespiratory reflexes mediated by nucleus tractus solitarii – a microinjection study in the rat. *J Physiol* **521**, 213–225.

Pickering AE & Paton JF (2006). A decerebrate, artificially-perfused in situ preparation of rat: Utility for the study of autonomic and nociceptive processing. *J Neurosci Methods* **155**, 260–271.

Pickering AE, Paton JFR, Harper AA & McAllen RM (2009). Central drives to cardiac ganglion neurons of rat: an intracellular analysis in situ. *Proc Physiol Soc* **15**, C6.

Pickering AE, Waki H, Headley PM & Paton JF (2002). Investigation of systemic bupivacaine toxicity using the in situ perfused working heart-brainstem preparation of the rat. *Anesthesiology* **97**, 1550–1556.

Rentero N, Cividjian A, Trevaks D, Pequignot JM, Quintin L & McAllen RM (2002). Activity patterns of cardiac vagal motoneurons in rat nucleus ambiguus. *Am J Physiol Regul Integr Comp Physiol* **283**, R1327–1334.

Richardson RJ, Grkovic I & Anderson CR (2003). Immunohistochemical analysis of intracardiac ganglia of the rat heart. *Cell Tissue Res* **314**, 337–350.

Rimmer K & Harper AA (2006). Developmental changes in electrophysiological properties and synaptic transmission in rat intracardiac ganglion neurons. *J Neurophysiol* **95**, 3543–3552.

Sampaio KN, Mauad H, Spyer KM & Ford TW (2003). Differential chronotropic and dromotropic responses to focal stimulation of cardiac vagal ganglia in the rat. *Exp Physiol* **88**, 315–327.

Seabrook GR, Fieber LA & Adams DJ (1990). Neurotransmission in neonatal rat cardiac ganglion in situ. *Am J Physiol Heart Circ Physiol* **259**, H997–1005.

Selyanko AA (1992). Membrane properties and firing characteristics of rat cardiac neurones in vitro. *J Auton Nerv Syst* **39**, 181–189.

Selyanko AA & Skok VI (1992). Synaptic transmission in rat cardiac neurones. *J Auton Nerv Syst* **39**, 191–199.

Simms AE, Paton JF & Pickering AE (2007). Hierarchical recruitment of the sympathetic and parasympathetic limbs of the baroreflex in normotensive and spontaneously hypertensive rats. *J Physiol* **579**, 473–486.

Sin PY, Webber MR, Galletly DC, Ainslie PN, Brown SJ, Willie CK, Sasse A, Larsen PD & Tzeng YC (2010). Interactions between heart rate variability and pulmonary gas exchange efficiency in humans. *Exp Physiol* **95**, 788–797.

Steele PA, Gibbins IL, Morris JL & Mayer B (1994). Multiple populations of neuropeptide-containing intrinsic neurons in the guinea-pig heart. *Neuroscience* **62**, 241–250.

Toader E, Cividjian A, Rentero N, McAllen RM & Quintin L (2008). Cardioinhibitory actions of clonidine assessed by cardiac vagal motoneuron recordings. *J Hypertens* **26**, 1169–1180.

Author contributions

Experiments were undertaken in the Pickering/Paton laboratory at the University of Bristol. Experiments designed and conceived by R.McA, J.F.R.P. and A.E.P.; all authors collected data; R.McA, L.M.S. and A.E.P. analysed data; all authors contributed to interpretation and drafting the manuscript.

Acknowledgements

We would like to thank Sandy Harper (University of Dundee) for triggering this investigation, and for thoughtful discussions and assistance with the identification of the gross ganglionic architecture. This study was supported by the British Heart Foundation. R.McA. was supported by NHMRC (Fellowship 232305 and Project grant 1010907). J.F.R.P. is in receipt of a Royal Society Wolfson Research Merit Award. A.E.P. is a Wellcome Trust Senior Clinical Fellow. The authors have no conflicts of interest.